Phytomedicine 143 (2025) 156824

Contents lists available at ScienceDirect

Phytomedicine

journal homepage: www.elsevier.com/locate/phymed

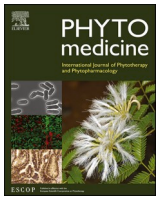

Original Article

Ponicidin promotes ferroptosis to enhance treatment sensitivity in Lenvatinib-resistant hepatocellular carcinoma cells through regulation of KEAP1/NRF2

Lisha Zhang [a,b,1], Hao Wang [c,1], Beibei Liang [a,d,1], Lijuan Qin [e], Mingzhu Zhang [f], Xingxian Lv [e], Shi Hu [g], Xiaoyu Fan [h], Wei Xie [a,d], Hao Yang [a], Gang Huang [a], Wei Jing [i,**], Jian Zhao [a,*]

[a] Shanghai Key Laboratory of Molecular Imaging, Jiading District Central Hospital Affiliated Shanghai University of Medicine and Health Sciences, Shanghai, PR China
[b] Nanchang Hongdu Hospital of TCM, Nanchang, PR China
[c] Department of Oncology, The Air Force Hosptital of Northern Theater PLA, Shenyang, China
[d] School of Pharmacy, Shanghai University of Medicine and Health Sciences, Shanghai, PR China
[e] Shanghai University of Traditional Chinese Medicine, Shanghai, PR China
[f] University of Shanghai for Science and Technology, Shanghai, PR China
[g] Department of Biomedical Engineering, College of Basic Medical Sciences, Second Military Medical University, Shanghai, PR China
[h] Department of Molecular Biology, Shanghai Center for Clinical Laboratory, Shanghai, PR China
[i] Department of Surgery, Changhai Hospital, Second Military Medical University, Shanghai, PR China

ARTICLE INFO

Keywords:
Hepatocellular carcinoma
Lenvatinib resistance
Ferroptosis
Ponicidin
KEAP1
NRF2

ABSTRACT

Objective: This study explores the therapeutic potential of Ponicidin on Lenvatinib-resistant hepatocellular carcinoma (HCC), elucidates its mechanism in reversing Lenvatinib resistance, and provides experimental evidence for its clinical application in overcoming this resistance.

Methods: Huh7 and HCC-LM3 cells were used to construct Lenvatinib-resistant cell lines, Huh7-LR and HCC-LM3-LR. Changes in the ferroptosis pathway post-drug resistance were observed by measuring ferroptosis-related markers. The proliferation assay were assessed by CCK-8, while the migration and invasion were measured by scratch and Transwell invasion assays. In mechanistic study, chip analysis and immunoprecipitation with biotin-labeled Ponicidin, were conducted to explore how Ponicidin overcame drug resistance. Xenograft model in nude mice was established to examine Ponicidin's anti-HCC effects *In vivo*. Clinical specimens were used to assess the true status of patients in Lenvatinib-resistant HCC patients.

Results: Our study reveals for the first time that ferroptosis inhibition drives Lenvatinib resistance in HCC and identifies Ponicidin as a novel KEAP1-targeting agent to reverse this process. In vitro, ferroptosis pathway was suppressed in Lenvatinib-resistant cells. Ponicidin suppressed proliferation, clonogenicity, migration, and invasion in these cells. The combination of Ponicidin and Lenvatinib significantly inhibited proliferation and reversed drug resistance by activating the ferroptosis pathway. Preliminary mechanistic studies showed that Ponicidin binds to KEAP1, stabilizing the KEAP1/NRF2 interaction, inhibiting the nuclear translocation and activation of NRF2, and thereby inducing ferroptosis to overcome Lenvatinib resistance. *In vivo*, the combination of Ponicidin and Lenvatinib exhibited a synergistic effect, significantly delaying tumor growth. Clinically, p-NRF2 and GPX4 expression was higher in the Lenvatinib-insensitive group, suggesting that the ferroptosis pathway was inhibited

Abbreviations: HCC, Hepatocellular carcinoma; VEGFR, Vascular endothelial growth factor receptor; FGFR, Fibroblast growth factor receptor; ROS, Reactive oxygen species; SLC7A11, Solute carrier family 7 member 11; GSH, Glutathione; GPX4, Glutathione peroxidase 4; NRF2/NFE2L2, nuclear factor erythroid 2-related factor 2; KEAP1, Kelch-like ECH-associated protein 1; ACSL4, Acyl-CoA Synthetase Long-Chain Family Member 4; LPCAT3, lysophosphatidylcholine acyltransferase 3; GEO, Gene Expression Omnibus; LR, Lenvatinib-resistant; MDA, Malondialdehyde; BCA, Bicinchoninic Acid; ECL, Enzyme-linked chemiluminescence; IHC, Immunohistochemistry; IF, Immunofluorescence; RI, Resistance indices; Co-IP, Co-immunoprecipitation; CHX, Cycloheximide; 4-OI, 4-Octyl Itaconate; CDX, Cell-derived xenograft.

* Corresponding author: Shanghai Key Laboratory of Molecular Imaging, Jiading District Central Hospital Affiliated Shanghai University of Medicine and Health Sciences, 279 Zhouzhu Road, Shanghai, PR China.
** Corresponding author: Department of Surgery, Changhai Hospital, Second Military Medical University, Shanghai, PR China.
E-mail addresses: jingwei77@smmu.edu.cn (W. Jing), j-zhao@vip.126.com (J. Zhao).
[1] Lisha Zhang, Hao Wang and Beibei Liang contributed equally to this work.

https://doi.org/10.1016/j.phymed.2025.156824
Received 6 December 2024; Received in revised form 17 April 2025; Accepted 29 April 2025
Available online 10 May 2025

in these patients. Thus, this study demonstrated that Ponicidin promotes ferroptosis to enhances treatment sensitivity in Lenvatinib-resistant HCC cells through KEAP1/NRF2.

Introduction

Hepatocellular carcinoma (HCC) stands as the second leading cause of cancer-related mortality globally, accounting for approximately 90 % of primary liver cancer cases (Llovet et al., 2016). In 2018, Lenvatinib, a multireceptor tyrosine kinase inhibitor, was approved as a first-line treatment for advanced HCC (Kudo et al., 2018). It exerts its anti-cancer activities by targeting multiple molecules, including vascular endothelial growth factor receptors 1–3 (VEGFR1–3), c-KIT/ stem cell factor receptor, RET and fibroblast growth factor receptors 1–4 (FGFR1–4) (Schlumberger et al., 2015). Despite substantial improvements in clinical outcomes, patients frequently experience cancer relapse due to Lenvatinib resistance. Potential mechanisms underlying this resistance include epithelial-mesenchymal transition, DNA damage response, autophagy, and RNA modification (Bo and Chen, 2023). Therefore, it remains crucial to investigate the mechanisms of Lenvatinib resistance and identify new therapeutic agents to overcome this challenge in HCC patients.

Ferroptosis represents an iron-dependent, lipid peroxidation-driven form of regulated cell death characterized by reactive oxygen species (ROS) overload (Dixon and Olzmann, 2024). Among its key regulatory components, the cystine-glutamate antiporter, known as system xCT (encoded by solute carrier family 7 member 11, SLC7A11 gene), imports cystine for the de novo synthesis of the antioxidant peptide glutathione (GSH) (Sanz et al., 2023). GSH, in turn, serves as a substrate for glutathione peroxidase 4 (GPX4), which catalyzes the detoxification of phospholipid hydroperoxides. GPX4 is a crucial negative regulator of ferroptosis by reducing lipid peroxidation (Pei et al., 2023). Both GPX4 and SLC7A11 are target genes of nuclear factor erythroid 2-related factor 2 (NRF2), a master transcription factor regulating numerous ferroptosis-related genes (Deng et al., 2024; Kerins and Ooi, 2018). NRF2 activity is mainly controlled by kelch-like ECH-associated protein 1 (KEAP1). Under normal conditions, NRF2 remains in the cytoplasm, bound to KEAP1 in an inactive complex. However, under ROS exposure or in the presence of electrophilic metabolites, the KEAP1 complex is inhibited, allowing NRF2 to dissociate from KEAP1 and translocate into the nucleus. There, NRF2 forms a heterodimer with small MAF proteins, initiating the antioxidant response by activating downstream target genes, ultimately inhibiting ferroptosis (Hirose et al., 2022).

The traditional Chinese medicinal plant *Rabdosia rubescens* (Hemsl.) has recently gained increasing interest in cancer treatment due to its favorable safety profile (Abdullah et al., 2021). Ponicidin (Rubescensine B), a tetracyclic diterpenoid derived from *R. rubescens*, exhibits potent anti-tumor activity. It has demonstrated significant anti-angiogenic effects and suppressed the proliferation of esophageal/colorectal cancer cells growth through multi-modal mechanisms including cell cycle arrest, apoptosis induction, and autophagy modulation (Zhang et al., 2019). Additionally, *R. rubescens* has been shown to regulate fatty acid metabolism and oxidative stress in non-alcoholic fatty liver disease. Notably, recent study revealed that Ponicidin exerts anti-proliferative effects in pancreatic cancer by triggering ferroptosis through dual modulation of the gamma-glutamyl cycle and polyunsaturated fatty acid metabolism (Cui et al., 2022).

The potential anti-HCC effects of Ponicidin and its relationship to ferroptosis induction remain to be fully elucidated. Here, we aimed to explore the impact of Ponicidin on Lenvatinib-resistant HCC cells and to assess the role of ferroptosis in this anti-tumor action.

Methods

Public RNA-seq datasets

RNA-seq data of the HCC cells was downloaded from the Gene Expression Omnibus (GEO) database (GSE211850), and 6 cell samples were screened. Log_2 (mRNA fold change) was used to assess differentially expressed mRNAs, with the calculated value of < -1 or > 1 deemed statistically significant (adj.$p < 0.05$). Then R package "pheatmap" and "ggplot2" were used to obtain ferroptosis-related genes heatmap and volcano plots.

Cell lines and reagents

Huh7 (Cat#: CTCC-003–0019), Huh7-LR (Cat#: CTCC-0521-NY) were obtained from Meisen Cell Technology Co., Ltd, (Zhejiang, China). HCC-LM3 was obtained from International Joint Cancer Institute, the Second Military Medical University (Shanghai, China). Ponicidin (Cat#: HY-N1535) and Lenvatinib (Cat#: HY-10,981) were purchased from MCE with purities of 99.82 % and 99.84 %, respectively. The chemical structures of Ponicidin and bio-Ponicidin are in Supplementary Fig. 3C.

Malondialdehyde (MDA) assay

1×10^6 cells/well of Huh7-LR and HCC-LM3-LR cells were seeded onto 6-well plates and treated with DMSO, 5 μM Lenvatinib, 15 μM Ponicidin, 15 μM Ponicidin-5 μM Lenvatinib combination, 15 μM Ponicidin-5 μM Lenvatinib plus Fer-1 for 24 h. For the measurement of MDA, 5×10^6 cells were collected and cleaned with ice-cold PBS to obtain cell precipitation, added 1 ml of pre-cooled Extraction Buffer. Cells were broken by ultrasonication in an ice bath for 5 min (power 20 % or 200 W, ultrasonication for 3 s, stop for 7 s, repeat 30 times). Centrifuged the cells at 13,000 g for 10 min at 4 °C, and took the supernatant for test using the MDA assay kits (Abbkine, Cat#: KTB1050).

GSH assay

Huh7-LR and HCC-LM3-LR cells were inoculated into 6-well plates with a cell density of 1×10^6 cells per well. These cells were subsequently treated with DMSO, 5 μM Lenvatinib, 15 μM Ponicidin, 15 μM Ponicidin - 5 μM Lenvatinib, a combination of 15 μM Ponicidin and 5 μM Lenvatinib along with Fer-1 incubated for 24 h. Then, collected 2×10^6 cells and cleaned the cells twice with ice-cold PBS (centrifuge at 4 °C for 10 min). Added 3 times the volume of Extraction Buffer and resuspended the cells. GSH levels in each experimental group were detected with the GSH kit (Abbkine, Cat#: KTB1600).

ROS assay

Huh7-LR and HCC-LM3-LR cells were seeded onto 6-well plates at a cell density of 1×10^6 cells per well. Subsequently, these cells were treated with DMSO, 5 μM Lenvatinib, 15 μM Ponicidin, 15 μM Ponicidin - 5 μM Lenvatinib, 15 μM Ponicidin - 5 μM Lenvatinib and Fer-1 cultured for 24 h. Diluted DCFH-DA probe (Beyotime, Cat#: S0033S) with FBS-free DMEM according to 1:1000 ratio, so that the final concentration reached 10 μM/l. Removed the original cell culture medium and add 1 ml of diluted DCFH-DA to each well, incubated at 37 °C for 20 min in a cell culture incubator. To completely eliminate the DCFH-DA that has not attached to the cells, the cells were washed three times using serum-free cell culture media. Lastly, a fluorescent microscope was used to

measure the ROS levels in each group.

Iron assay

The iron assay kit (Abcam, Cat#: ab83366) was used to measure the iron level. Huh7-LR and HCC-LM3-LR cells were plated (1×10^6 cells/well) in 6-well plates and treated with Ponicidin and Lenvatinib for 24 h at different concentrations. Harvested cells (2×10^6 cells) were homogenized in 4–10 vol Iron Assay buffer. Centrifuged (16,000 g, 10 min, 4 °C) to pellet debris. Adjusted supernatant tof 100 µl with Iron Assay Buffer. Sample wells of a 96-well plate were filled with 1–50 µl samples to test ferrous iron, and the volume was increased to 100 µl each well using Assay Buffer. 5 µl of iron assay buffer was added to every sample.

Immunoprecipitation and pull-down assay

Huh7-LR cell was seeded onto 6-well plates at a cell density of 1×10^6 cells per well. The cell was treated with 15 µM Bio-Ponicidin for 6 hours. For the endogenous interaction assay, Huh7-LR was stimulated and lysed with lysis buffer and the cell lysate was incubated at 4 °C overnight with the streptavidin magnetic bead conjugate (Cell Signaling Technology, Cat#: 5947S). The proteins bound by Ponicidin were pulled down by streptavidin beads and subjected to immunoblotting analysis.

Animal studies and images

Male athymic BALB/c nude mice (4-weeks old) were purchased from Shanghai Jihui Laboratory Animal Care Co., Ltd. (Shanghai, China). Mice were specific pathogenfree, maintained under a strict 12 h light cycle (lights on at 07:00 a.m. and off at 07:00 pm.). Huh7-LR cells were cultivated until they reached 5×10^7 cells per milliliter. The nude mice's backs were then infected with 5 × 106 cells in a 100µl volume. The mice were divided into five groups at random once the tumors' average volume reached 100 mm^3. Six groups (each group, n = 5) were treated as follows: control group: DMSO; Lenvatinib group: 10 mg/kg Lenvatinib; Ponicidin group: 10 mg/kg and 20 mg/kg Ponicidin; Lenvatinib - Ponicidin group: 10 mg/kg Lenvatinib combine with 10 mg/kg or 20 mg/kg Ponicidin. ntragastric once a day, the combined group within a day interval of 6 h, give medicine for 28 days. Vernier calipers were used to measure the tumor volume of naked mice every five days. Tumor volume was calculated as 0.5 × (Length × Width2), where l and W represent the long and short diameter, respectively. The mice were sacrificed after 28 days.

Statistical analysis

The mean ± standard deviation of a minimum of three repeated samples was used to express the group results. GraphPad Prism and SPSS statistical software (SPSS, Chicago, IL, USA) were used to assess the differences between the groups. Independent sample *t*-test or oneway analysis of variance (ANOVA) were as necessary, with $p < 0.05$ being statistically significant.

Result

Ferroptosis resistance occurred in Lenvatinib-resistant cells

To identify the differential genes associated with Lenvatinib resistance in HCC, we first performed RNA-seq analysis to compare expression levels between three Lenvatinib-resistant and parental Huh7 cells based on GSE186191. The heatmap showed the expression of 14 ferroptosis-related genes (Fig. 1A). Among the differentially expressed genes, SLC7A11 and NRF2 were significantly upregulated in Lenvatinib-resistant Huh7 cells. Volcano plots yielded consistent results (Fig. 1B). GPX4, an important protein for cellular lipid peroxide scavenging and a key regulator of ferroptosis, also showed a significant increase despite an adjusted p-value (adj.P) of <0.05 (Fig. 1B). qRT-PCR showed that the expression of SLC7A11, NRF2, GPX4 and 11 ferroptosis-related genes in RNA-seq analysis significantly changed in Lenvatinib-resistant Huh7 (Fig. 1C and Supplementary Fig. 1).

To verify ferroptosis resistance, we constructed Lenvatinib-resistant Huh7 and HCC-LM3 cell lines. The resistance indices (RI) of Huh7-LR and HCC-LM3-LR were 4.81 and 2.03, respectively (Fig. 1D). Lipid peroxidation, a hallmark of ferroptosis, produces the cytotoxic end product malondialdehyde (MDA), which cross-links and polymerizes macromolecules such as proteins and nucleic acids. Our results showed that MDA levels decreased in Lenvatinib-resistant Huh7 and HCC-LM3 cells (Fig. 1E). GSH, an important intracellular antioxidant that scavenges lipid peroxides via glutathione peroxidase, was significantly elevated in these cells (Fig. 1F). However, there was no change in Fe^{2+} content between the two groups (Fig. 1G).

ROS, chemically reactive molecules containing oxygen, are natural by-products of cellular metabolism. The ROS assay showed a decrease in ROS levels in Lenvatinib-resistant Huh7 and HCC-LM3 cells (Fig. 1H). These results aligned with the initial heatmap data, indicating that ferroptosis resistance occurs in Lenvatinib-resistant Huh7 and HCC-LM3 cells.

Ponicidin significantly inhibited proliferation, migration, and invasion of in Lenvatinib-resistant HCC cells

Ponicidin (Rubescensine B), derived from *R. rubescens*, was reported to suppress cancer cell growth by inducing apoptosis (Du et al., 2015; Liu et al., 2006) or ferroptosis (Cui et al., 2022). However, the effects of Ponicidin on Lenvatinib-resistant HCC cells hasn't been explored. To explore the effects of Ponicidin on Lenvatinib-resistant HCC cells, we used the CCK-8 assay to measure the proliferation of Lenvatinib-resistant Huh7 (Huh7-LR) and HCC-LM3 (HCC-LM3-LR) cells over 24, 48, and 72 hours at varying Ponicidin concentrations. The results demonstrated that Ponicidin significantly inhibited the growth of both Huh7-LR (Fig. 2A) and HCC-LM3-LR cells (Fig. 2B). In contrast, no cytotoxicity was observed in human embryonic hepatocytes (HHL-5) at the same concentrations (Fig. 2C). We then assessed the impact of Ponicidin on the clonogenic ability of Lenvatinib-resistant HCC cells. After treatment with different concentrations of Ponicidin, the number of clone-forming colonies was significantly reduced, confirming that Ponicidin inhibited the proliferation of Huh7-LR and HCC-LM3-LR cells (Fig. 2D).

Tumor cells possess strong migratory and invasive capabilities. We next investigated the effects of Ponicidin on these characteristics. Scratch assay results showed that 10 µM and 15 µM Ponicidin significantly inhibited the migration of Huh7-LR and HCC-LM3-LR cells (Fig. 2E). Similarly, the Transwell invasion assay indicated that Ponicidin at 10 µM and 15 µM inhibited the invasion of both cell lines (Fig. 2F). These findings suggest that Ponicidin exerts anti-tumor effects on Lenvatinib-resistant HCC cells by inhibiting proliferation, migration, and invasion.

Ponicidin induced cell death via the ferroptosis pathway

To determine the pathway by which Ponicidin induces cell death, we assessed HCC-LM3-LR proliferation in the presence of various cell death inhibitors, including the apoptosis inhibitor Z-VAD-FMK, the ferroptosis inhibitor Fer-1, the autophagy inhibitor CQ, and the necrosis inhibitor Nec-1 (Fig. 3A). The results demonstrated that cell viability was significantly restored upon the addition of Z-VAD-FMK and Fer-1, indicating that Ponicidin exerted its anti-Lenvatinib-resistant effects on HCC via both the ferroptosis and apoptosis pathways. To further confirm the inhibitory effects of Ponicidin on other hepatocellular carcinoma cells, we evaluated the clone formation ability of several HCC cell lines, including MHCC-97H, SNU449, SNU398, Huh7, Huh7-LR, HCC-LM3, HCC-LM3-LR, and Hep-G2 (Fig. 3B). The results revealed that most HCC

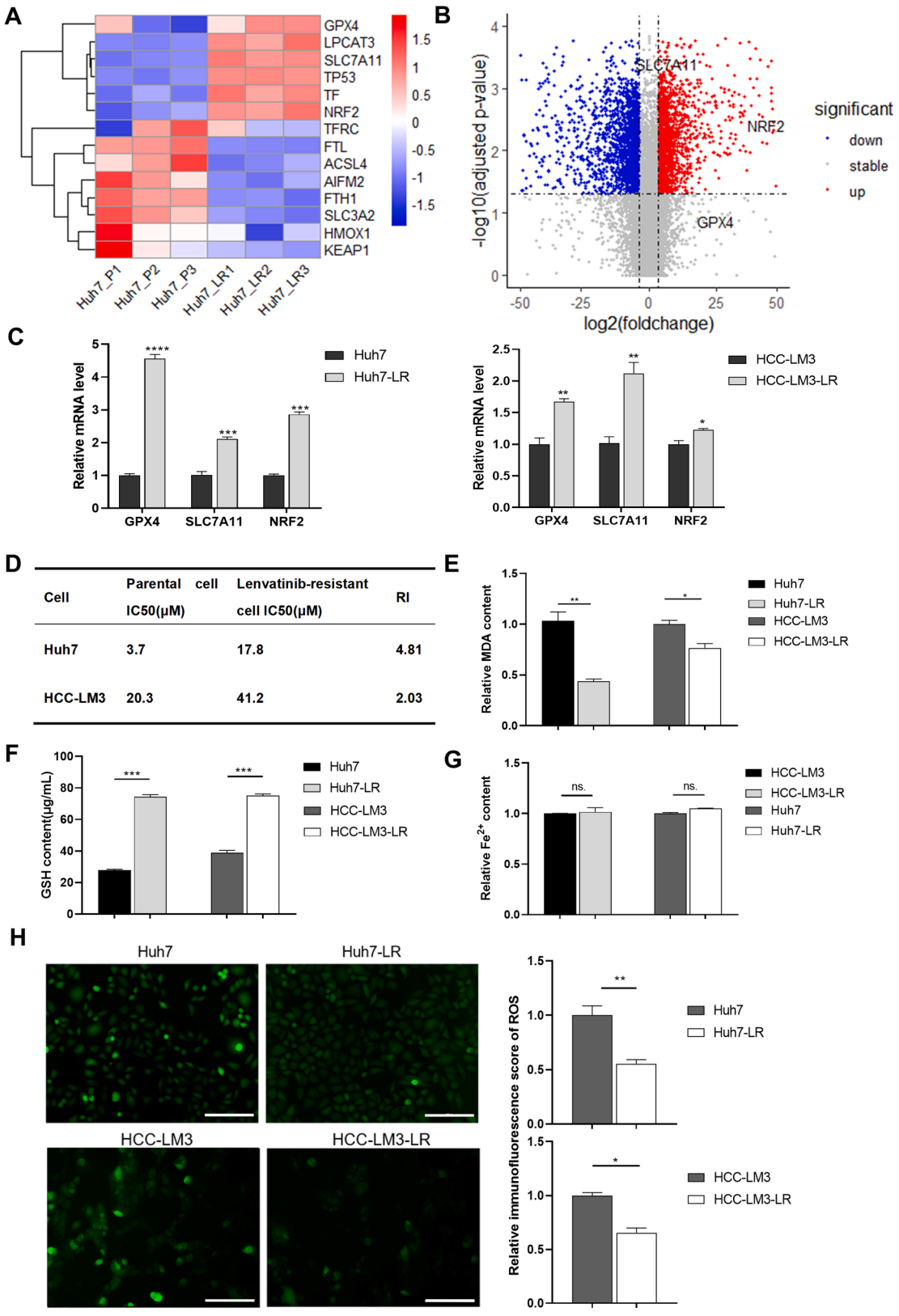

Fig. 1. Ferroptosis resistance occurred in Lenvatinib-resistant cells. (A)Heatmap of 14 ferroptosis-related genes in based on GSE186191. (B)Volcano plots with differentially expressed genes in Lenvatinib-resistant Huh7 vs. parental Huh7 cells. (C) qRT-PCR assay for GPX4, SLC7A11, and NRF2 mRNA levels in Huh7 and Huh7-LR, HCC-LM3 and HCC-LM3-LR cells. (D)Huh7 and HCC-LM3 cells' resistance index met experimental requirements after sustained induction of Lenvatinib for 6 months. (E-H) MDA(E), GSH(F), Fe^{2+}(G) and ROS(H) levels in parental and Lenvatinib-resistant cells of Huh7 and HCC-LM3 were detected by kits. Scale bar: 200 μm, $*p < 0.05$; $**p < 0.01$; $***p < 0.001$; $****p < 0.0001$.

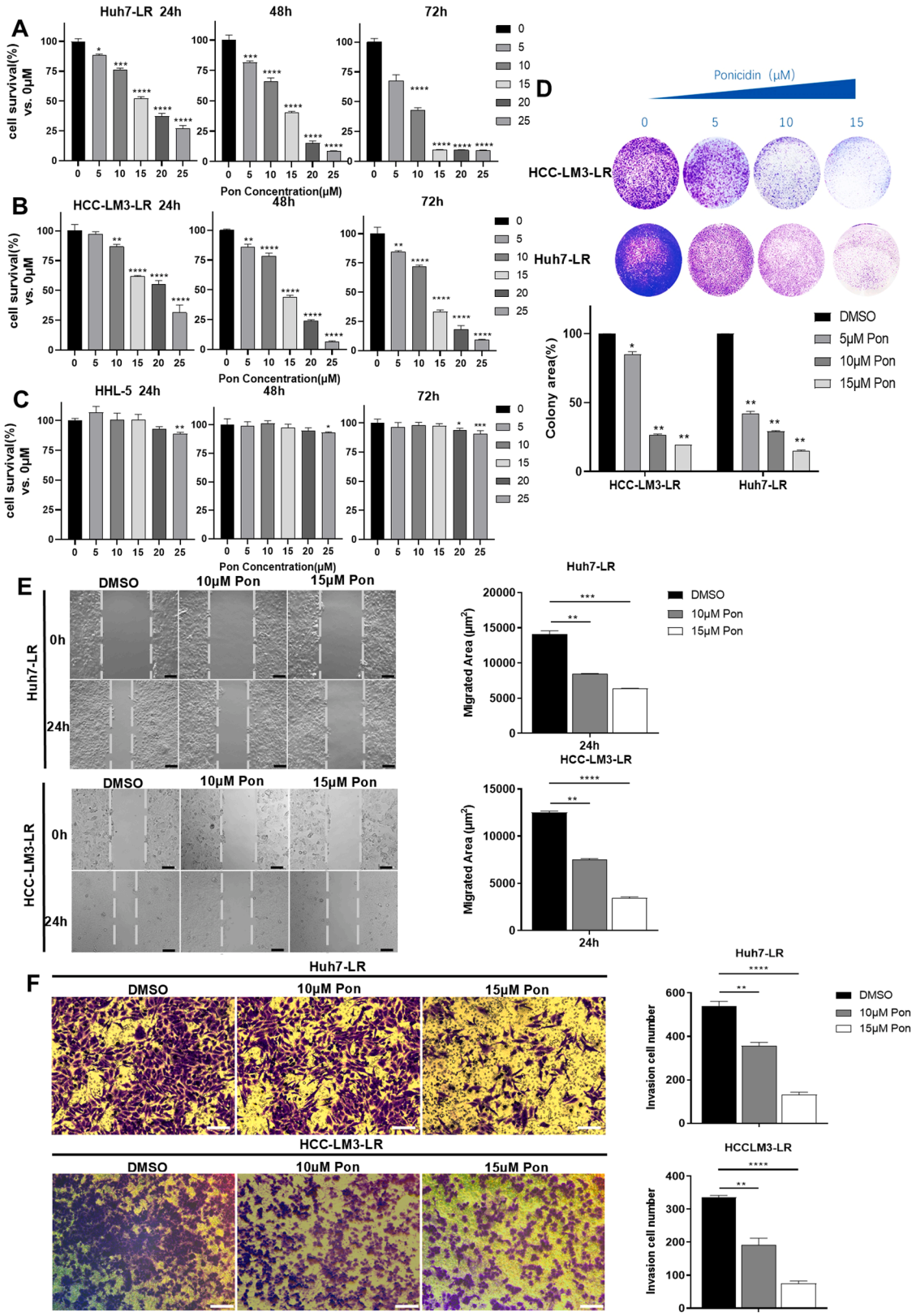

Fig. 2. Ponicidin significantly inhibited proliferation, migration, and invasion of in Lenvatinib-resistant HCC cells. (A-C) Huh7-LR(A), HCC-LM3-LR(B), HHL5(C) cells were plated into a 96-well cell culture plate with a clear bottom, seeded 2000 cells per well for cell proliferation assay. Added 10 % of CCK-8 Solution into cells and incubate for one hour after 24–72 hours of 5–25 μM Ponicidin treatment. After 5–25 μM Ponicidin was applied to Huh7-LR and HCC-LM3-LR cells for 24–72 h. (D) 2×10^3 Huh7-LR and HCC-LM3-LR cells were cultured in 6-well plates per well for 24 h, then cultured in medium containing 20 % FBS for 14d Colony number (down) and representative image was taken. (E)Wound healing assay and migration areas of treated Huh7-LR and HCC-LM3-LR cells. (F) Huh7-LR and HCC-LM3-LR cells cultured with Matrigel in the upper chamber of the Transwells. 15 μM Pon was added to the cells. 20 % serum containing medium was add to the bottom wells. After cultured 22–26 h, counted invading cells by a light Microscope. Scale bar: 200 μm;*$p < 0.05$; **$p < 0.01$; ***$p < 0.001$; ****$p < 0.0001$.

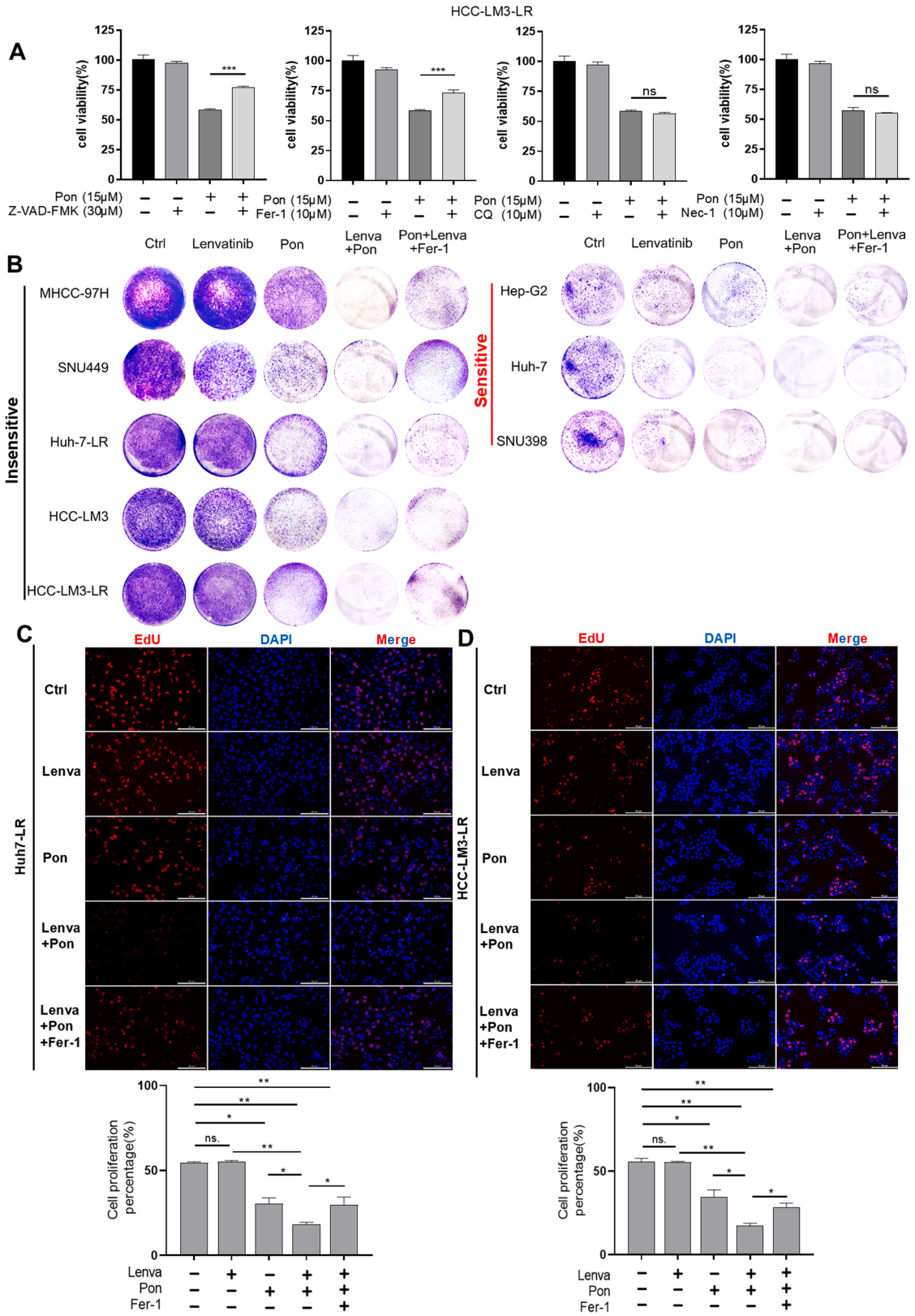

Fig. 3. Ponicidin induced cell death via the ferroptosis pathway. (A) HCC-LM3-LR cells were pretreated overnight with 30 μM Z-VAD-FMK, 10 μM ferrostatin-1 (Fer-1), 10 μM chloroquine (CQ) and 10 μM necrostatin-1 (Neo-1), then treated with 15 μM Ponicidin for 24 hours (average of three replicates). (B) 2×10^3 MHCC97H, SNU449,SNU398,Huh7,Huh7-LR,HCC-LM3,HCC-LM3-LR,Hep-G2 cells were cultured in 6-well plates per well added DMSO, 10 μM Lenvatinib (Lenva), 15 μM Ponicidin (Pon), 15 μM Pon+10 μM Lenva, 15 μM Pon+10 μM Lenva+10 μM Fer-1 for 24 h, then cultured in medium containing 20 % FBS for 14d (C, D) Huh7-LR and HCC-LM3-LR cells were seeded onto 6-well plates at a cell density of 1×10^6 cells per well. Subsequently, these cells were treated with DMSO, 5 μM Lenva, 15 μM Pon, 15 μM Pon + 5 μM Lenva, 15 μM Pon + 5 μM Lenva + 10 μM Fer-1 cultured for 24 hours. The proliferation ability of cells was measured by EdU kit. Scale bar: 200 μm. $^*p < 0.05$; $^{**}p < 0.01$; $^{***}p < 0.001$; $^{****}p < 0.0001$.

cells were naturally resistant to Lenvatinib, with only a subset showing better sensitivity, explaining the generally poor prognosis of HCC. Ponicidin alone significantly inhibited the clone formation ability of Lenvatinib-resistant HCC cells, particularly MHCC-97H, SNU449, HCC-LM3, Huh7-LR, and HCC-LM3-LR. The combination of Lenvatinib and Ponicidin produced an even stronger inhibitory effect on clone formation, exhibiting a notable synergistic effect. This effect was partially reversed by Fer-1, confirming the role of ferroptosis in Ponicidin-mediated cell death. Then we choose Gefitinib as a positive control, which has been reported to overcome Lenvatinib resistance in EGFR-positive HCC cells (Jin et al., 2021). We compared the effects of Gefitinib and Ponicidin on EGFR-positive Huh7-LR cells. The results showed that Ponicidin had the similar efficacy with that of Gefitinib on inhibition of cell proliferation as detected by cloning assay, when combination with Lenvatinib (Supplementary Fig. 2). We also used the EdU assay to assess the impact of Ponicidin and Lenvatinib on DNA replication, reflecting cell proliferation (Fig. 3C and D). The results showed that while Lenvatinib alone did not inhibit DNA replication, Ponicidin alone could efficiently inhibit DNA replication. The combination treatment significantly suppressed DNA replication, an effect that was partially or completely reversed by Fer-1. These results indicate that Ponicidin induces cell death via the ferroptosis pathway in Lenvatinib-resistant HCC cells.

Ponicidin sensitized Lenvatinib-resistant HCC cells to ferroptosis

To further investigate whether Ponicidin induces cell death through the ferroptosis pathway, we selected Huh7-LR and HCC-LM3-LR cells and measured ferroptosis markers, including GSH, MDA, Fe^{2+}, and ROS. The results showed that GSH levels (Fig. 4A) were significantly reduced, while intracellular MDA (Fig. 4B), Fe^{2+} (Fig. 4C), and ROS levels (Fig. 4D and 4E) were significantly increased in the Ponicidin-alone and combination treatment groups. These effects were partially or completely reversed by Fer-1, indicating that the cells were undergoing ferroptosis after Ponicidin treatment.

In addition, ferroptosis is characterized morphologically by markedly shrunken mitochondria with significantly increased membrane densities, severely fragmented or absent cristae, and ruptured outer mitochondrial membranes, accompanied by a pronounced decline or complete loss of mitochondrial membrane potential (Xie et al., 2016). JC-1, an optimal fluorescent probe for detecting mitochondrial membrane potential during early cell death, a hallmark of early apoptosis (Perelman et al., 2012), was used to assess the ferroptosis state (Yang et al., 2024). The results demonstrated that the mitochondrial membrane potential in Huh7-LR and HCC-LM3-LR cells treated with Ponicidin alone was significantly decreased, while the potential in the combination treatment group was almost completely lost. This effect was reversed by Fer-1 (Fig. 4F). These findings further confirm that Ponicidin induces ferroptosis, thereby re-sensitizing Lenvatinib-resistant cells.

Ponicidin directly bound to KEAP1 and stabilized KEAP1-NRF2 interaction

To further investigate the mechanism of Ponicidin-induced ferroptosis in Lenvatinib-resistant cells, qRT-PCR was conducted to detect key ferroptosis-related genes. The results showed that mRNA levels of GPX4 and NRF2 were significantly downregulated, while ACSL4 and LPCAT3, crucial regulators in lipid metabolism and ferroptosis were significantly upregulated in Huh7-LR and HCC-LM3-LR cells treated with Ponicidin, suggesting that Ponicidin induced ferroptosis (Fig. 5A). To better detect ferroptosis occurrence, we performed a time-gradient experiment. The results showed that GPX4 levels were lowest when 15 μM Ponicidin was applied for 24 hours, indicating that most cells were undergoing ferroptosis at that time (Fig. 5B). We also examined GPX4 and SLC7A11 expression at different Ponicidin concentrations (Fig. 5C). The results confirmed that Ponicidin induced ferroptosis in Huh7-LR and HCC-LM3-LR by downregulating GPX4 and SLC7A11, with a significant dose-dependent effect.

Lower binding energies indicate stronger interactions between components and their targets, so we selected ferroptosis-related proteins with binding energies ≤ -5.0 kcal/mol for target screening. Molecular docking results revealed that Ponicidin could bind to GPX4, SLC7A11, and KEAP1 (Fig. 5D, Supplementary Fig. 3 and Supplementary Table 1). To identify which ferroptosis-related protein Ponicidin binds to, we constructed biotin-labeled Ponicidin (Bio-Pon, Supplementary Fig. 4) and used the HuProt™ Human Proteome Microarray to screen for ferroptosis-related proteins binding to Bio-Pon (Supplementary Fig. 5A and Supplementary Table 2). Molecular docking and microarray analysis suggested that KEAP1 was a likely binding target for Ponicidin. Immunofluorescence assays further validated this finding, showing that Bio-Pon and KEAP1 co-localized in the cytoplasm (Fig. 5E). Co-Immunoprecipitation (Co-IP) results confirmed that Bio-Pon could pull down KEAP1 and a small portion of NRF2, while enhancing KEAP1 expression, indicating that Ponicidin directly binds to KEAP1 (Fig. 5F and Supplementary Fig. 5B).

To explore the impact of Ponicidin binding with KEAP1, we performed western blot analysis on Huh7-LR cells treated with cycloheximide (CHX) and MG132 to determine KEAP1 protein stability. The results indicated that Ponicidin could slow the KEAP1 degradation (Fig. 5G). KEAP1 functions as an NRF2 inhibitor, binding to NRF2 and retaining it in the cytoplasm. Phosphorylated NRF2 (p-NRF2, Ser40), the activated form of NRF2, can enter the nucleus and promote the expression of downstream genes like SLC7A11 and GPX4. To observe how Ponicidin affects NRF2, we conducted western blot analysis on Huh7-LR cells treated with DMSO, Ponicidin, the NRF2 inhibitor ML385, and the NRF2 inducer 4-Octyl Itaconate (4-OI). The results showed that Ponicidin significantly increased KEAP1 expression and inhibited NRF2 expression and activation. ML385 had a similar but less pronounced effect, while 4-OI exhibited the opposite effect (Fig. 5H). We also performed nucleocytoplasmic separation assays in the same groups, which revealed that Ponicidin significantly inhibited NRF2 activation and SLC7A11 expression. Similar effects were observed with ML385, while both p-NRF2 and SLC7A11 were highly expressed with 4-Octyl Itaconate (Fig. 5I). Additionally, immunofluorescence assays showed that KEAP1 fluorescence intensity increased, and KEAP1-NRF2 binding was tighter (Fig. 5J). These results suggest that the anti-tumor and drug-resistance reversal effects of Ponicidin may be due to its enhancement of KEAP1-NRF2 binding, which hinders NRF2 translocation to the nucleus and its activation.

Expression of KEAP1/NRF2/GPX4 in Lenvatinib-resistant mouse xenograft tumor models and patients

To explore the role of Ponicidin *In vivo*, we used nude mice to establish a Huh7-LR cell-derived xenograft (CDX) model. The results indicated that tumor volume was smaller in the Ponicidin-treated group, suggesting that Ponicidin alone effectively inhibited tumor growth. The tumor volume in the combination group was significantly reduced, demonstrating the synergistic effect of Lenvatinib and Ponicidin (Fig. 6A). Immunohistochemical staining was then performed to examine the expression of KEAP1, p-NRF2, and GPX4 in tumor tissues. The results showed that KEAP1 expression was upregulated in both the Ponicidin and combination groups, with the highest expression in the combination group, whereas p-NRF2 and GPX4 protein expression was significantly downregulated, consistent with the in vitro findings (Fig. 6B).

To assess the true situation of these indicators in the clinic, we collected 59 clinical specimens from HCC patients treated with Lenvatinib and divided them into Lenvatinib-sensitive and Lenvatinib-insensitive groups, based on recurrence time ($\leq$ 1 year: Lenvatinib-insensitive group; $>$ 1 year: Lenvatinib-sensitive group). Then we used

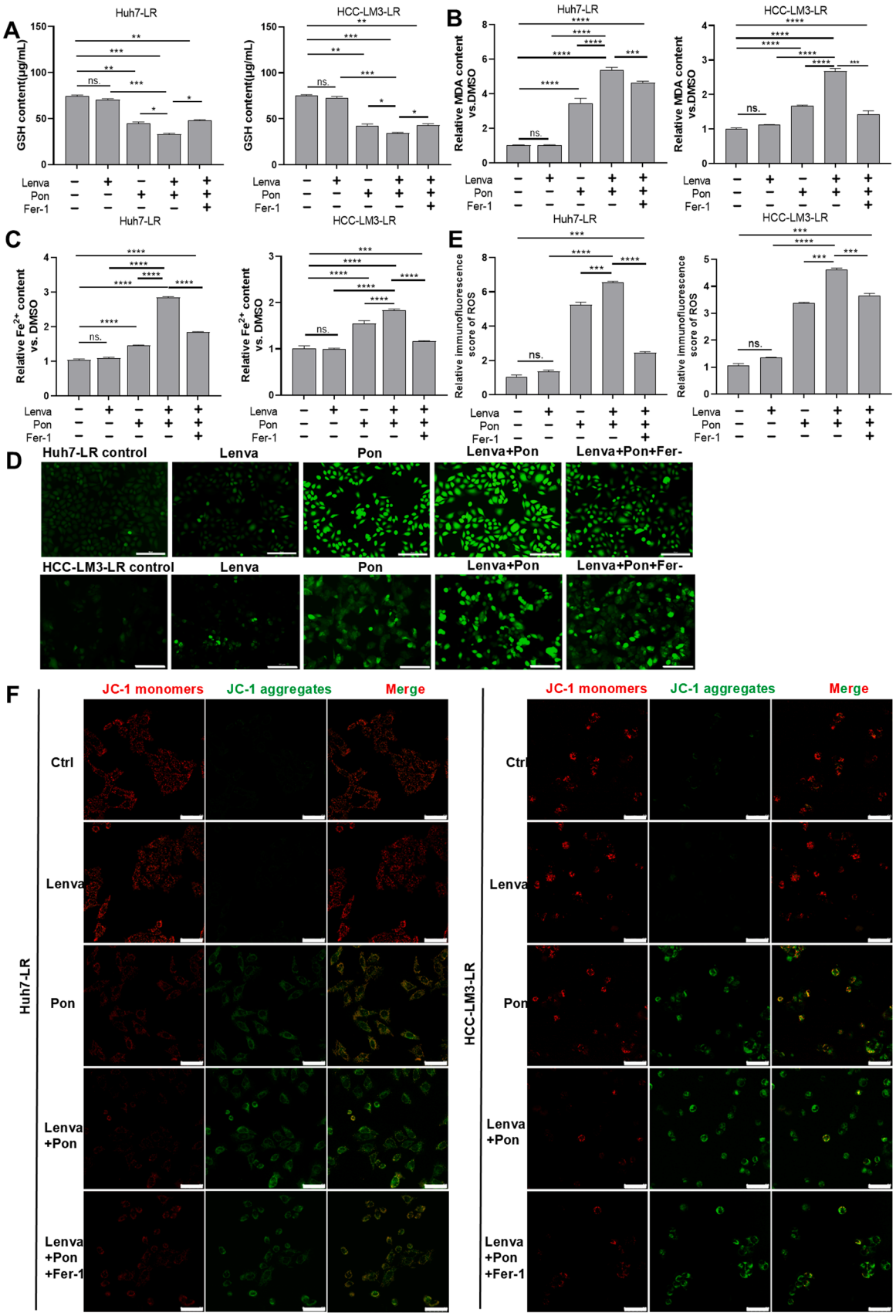

Fig. 4. Ponicidin sensitized Lenvatinib-resistant HCC cells to ferroptosis. (A-C) Huh7-LR and HCC-LM3-LR cells were treated with DMSO, 10 μM Lenva, 15 μM Pon, 15 μM Pon+10 μM Lenva, 15 μM Pon+10 μM Lenva+10 μM Fer-1 for 24 h, then cells were collected and used assay kits for GSH(A), MDA(B), Fe^{2+}(B) content detection. (D-E) ROS content was detected by fluorescence microscopy in Huh7-LR and HCC-LM3-LR cells. Scale bar: 200 μm. (F) Mitochondrial membrane potential was analyzed by kit with JC-1, observed by confocal microscopy. Scale bar: 50 μm, $^{*}p < 0.05$; $^{**}p < 0.01$; $^{***}p < 0.001$; $^{****}p < 0.0001$.

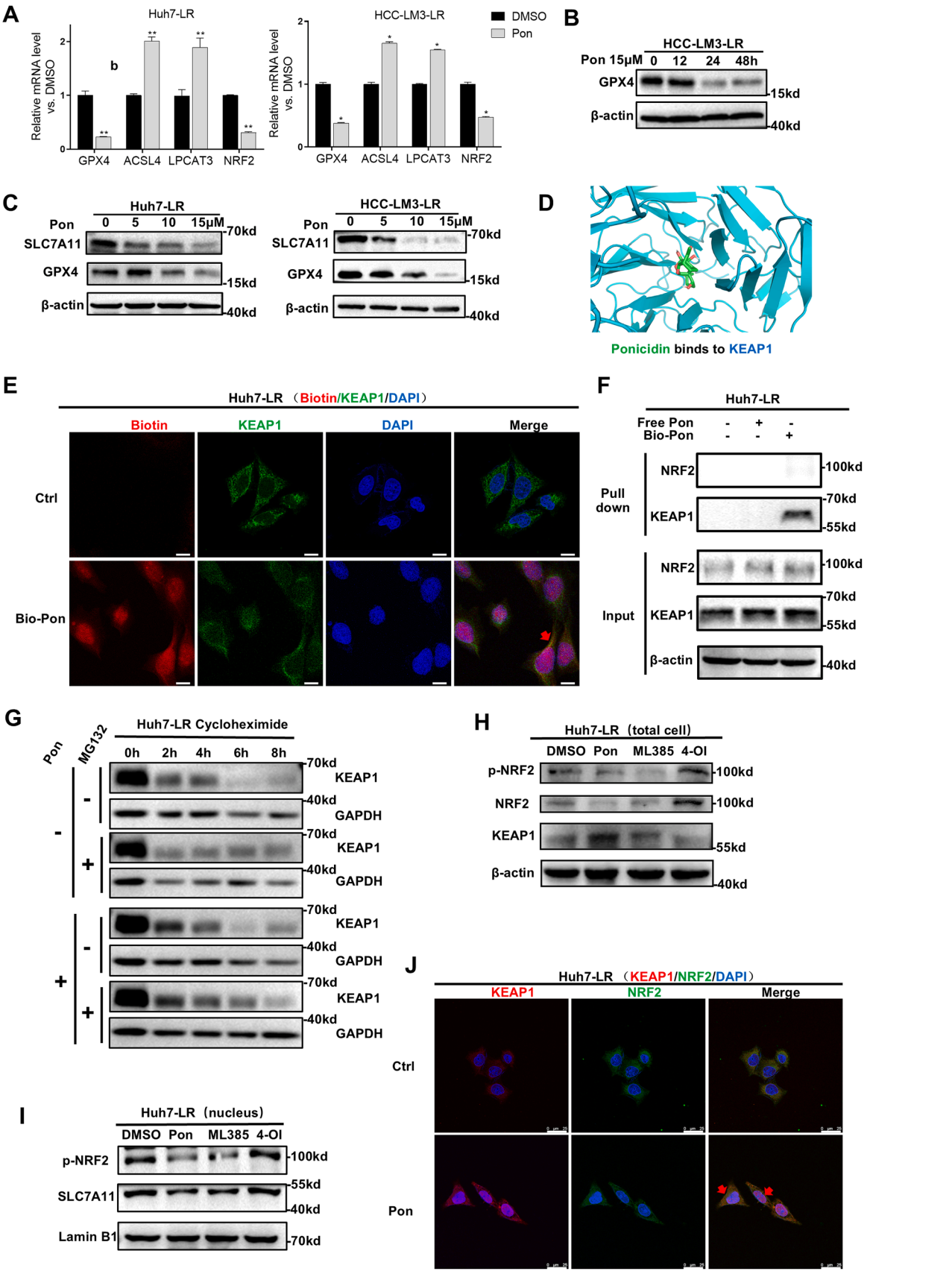

(caption on next page)

Fig. 5. Ponicidin directly bound to KEAP1 and stabilized KEAP1-NRF2 interaction. (A) Huh7-LR and HCC-LM3-LR cells after Ponicidin treatment were used for validation at the mRNA level. (B) Western blot analysis of HCC-LM3-LR cells treated with 15 μM Ponicidin in different hours. (C) Western blot analysis of Huh7-LR and HCC-LM3-LR cells treated with the indicated concentrations of Ponicidin. (D) The result of Ponicidin and KEAP1 molecular docking. (E) The cells were immunostained for Bio-Pon(red), KEAP1(green), and DNA (DAPI, blue). Representative fluorescence images of Bio-Pon and KEAP1 anchored as shown. Scale bar: 50 μm. (F) Huh7-LR cells were co-incubated with Bio-Pon for 6 h for protein extraction, which were then pulled down using streptavidin beads. The total proteins (Input) and bound proteins (Pull down) immunoblotted as indicated. (G) Huh7-LR cells were co-incubated with 50μg/ml cycloheximide (CHX) for 0,2,4,6,8 h with or not with Ponicidin and 30μ M MG132. KEAP1 and GAPDH were detected by Western blotting. (H-I) The effect Ponicidin, ML385, 4-Octyl Itaconate on the expression of ferroptosis-related proteins in total cell (H) and nucleus (I) were detected by Western blotting. (J) Huh7-LR cells as indicated were subjected to immunofluorescence staining of KEAP1(red), NRF2(green), and DNA (DAPI, blue). Scale bars: 50 μm.

immunohistochemical staining to assess KEAP1, p-NRF2, and GPX4 expression. The results indicated that p-NRF2 and GPX4 expression was higher in the Lenvatinib-insensitive group, while KEAP1 expression was slightly higher but not statistically different, suggesting that the NRF2-GPX4 mediated anti-ferroptosis pathway was activated in these patients (Fig. 6C). The correlation in clinic pathologic parameters in all HCC patients was statistically analyzed (Table 1). Significant correlations between Lenvatinib sensitivity and age ($p = 0.003$), AFP level ($p = 0.005$) or AJCC stage ($p = 0.002$) were observed. Importantly, significant correlations between Lenvatinib sensitivity and GPX4 ($p = 0.000$) or p-NRF2 ($p = 0.004$) expression levels were observed. In contrast, this correlation was not statistically significant in the KEAP1 expression ($p = 0.959$). No significant correlation was found between Lenvatinib sensitivity and other variables, including sex, tumor volume, or cirrhosis. In univariate analysis, age, AFP, AJCC stage, GPX4, and p-NRF2 expression status are to be prognostic factors for RFS ($P < 0.05$, Supplementary Table 3). These findings showed that activation of NRF2 and GPX4 occurred in Lenvatinib-resistant patients, indicating that the ferroptosis pathway was inhibited in the context of Lenvatinib resistance.This inhibition was reversed by Ponicidin in Huh7-LR CDX model.

Discussion

HCC is one of the most prevalent and devastating causes of cancer-related deaths worldwide. Approximately 70 % of HCC patients present with advanced disease at diagnosis, limiting opportunities for radical treatment (Qin et al., 2024). For these patients, Lenvatinib is a standard-of-care therapy, targeting cancer cells by inhibiting multiple receptor tyrosine kinases. However, resistance to therapy presents a significant clinical challenge across various therapeutic approaches (Ladd et al., 2024). While some mechanisms involved in the development of Lenvatinib resistance are known, many others remain largely unexplored. Our study provides the first evidence that ferroptosis suppression, mediated by the KEAP1/NRF2/GPX4 axis, is a hallmark of acquired Lenvatinib resistance in HCC, a finding not previously reported in the context of tyrosine kinase inhibitor (TKI) resistance. This study converges with accumulating evidence demonstrating that evasion of ferroptosis underlies therapeutic resistance (Li et al., 2024), while uniquely uncovering NRF2-mediated antioxidant remodeling as a central molecular determinant driving hepatocellular carcinoma progression.

In the past decade, ferroptosis has emerged as a critical pathway in many types of tumors (Lei et al., 2022). Unlike apoptosis, necrosis, and autophagy (Hassannia et al., 2019; Zhang et al., 2022), ferroptosis is characterized by the iron-dependent accumulation of lethal lipid ROS (Huang et al., 2023). Enhancing ferroptosis could significantly increase the cancer cell-killing effect. Iseda N et al. (Iseda et al., 2022) found that Lenvatinib suppresses GPX4 expression by reducing cystine import activity, which leads to lipid ROS accumulation. Silencing FGFR4 further reduced GPX4 expression and increased lipid ROS levels. Moreover, activation of NRF2 also suppressed ferroptosis through ROS accumulation, and NRF2 inhibitors were shown to enhance Lenvatinib efficacy. These findings suggest that ferroptosis contributes to the therapeutic effects associated with Lenvatinib. As Lenvatinib triggers ferroptosis, resistance mechanisms likely evolve into acquired drug resistance. In our study, we aimed to elucidate the molecular drivers of Lenvatinib resistance by combining transcriptomic analysis with cellular experiments. Our results showed reduced MDA content and increased ROS and GSH levels in Lenvatinib-resistant HCC cells, suggesting that ferroptosis was suppressed in these cells.

Ponicidin, a novel KEAP1-targeting agent extract derived from the traditional Chinese herb *Rabdosia rubescens*, has been reported to exert anti-tumor effects in various cancers (Islam et al., 2019). In this study, we explored the potential of Ponicidin as a therapeutic agent for Lenvatinib-resistant HCC. We demonstrated that Ponicidin inhibited the growth, migration, and invasion of Lenvatinib-resistant HCC cells in vitro. To determine the cell death pathway mediated by Ponicidin, we added several cell death inhibitors, including the apoptosis inhibitor Z-VAD-FMK, the ferroptosis inhibitor Fer-1, the autophagy inhibitor CQ, and the necrosis inhibitor Nec-1. We found that cell viability was significantly restored with the addition of Z-VAD-FMK and Fer-1, suggesting that Ponicidin exerted its effects through ferroptosis and apoptosis pathways. Our results showed that GSH content was significantly reduced, while intracellular MDA, Fe^{2+}, and ROS levels were significantly increased, mitochondrial membrane potential was decreased in both the Ponicidin-alone and the Ponicidin-Lenvatinib combination groups, which could be reversed by Fer-1. These findings suggest that Ponicidin induces ferroptosis, thereby re-sensitizing Lenvatinib-resistant cells.

Ferroptosis induces specific mitochondrial morphological changes distinct from other forms of cell death (Javadov, 2022). Cells exposed to ferroptotic stimuli, such as erastin or RSL3, exhibit fragmented, high-density, compact mitochondria with ruptured outer membranes and disorganized or lost cristae (Jang et al., 2021). Similarly, GPX4 silencing increased the number of swollen mitochondria with a lamellar architecture and reduced cristae (Friedmann Angeli et al., 2014). Ferroptosis affects various aspects of mitochondrial metabolism and quality control mechanisms, including mitochondrial biogenesis, dynamics, and mitophagy (Basit et al., 2017; Song et al., 2021). JC-1, an ideal fluorescent probe for detecting mitochondrial membrane potential during early cell death, was used to assess ferroptosis. Our results showed that the mitochondrial membrane potential of Lenvatinib-resistant HCC cells treated with Ponicidin alone was significantly decreased, and the membrane potential in the Ponicidin and Lenvatinib combination group was almost completely lost. In accordance with this finding, the expressions ASCL4 and LPCAT3, crucial regulators of lipid peroxidation and ferroptosis, were greatly enhanced upon Ponicidin adminstration. In the process of ferroptosis, ACSL4 activates polyunsaturated fatty acids to acyl-CoA, LPCAT3 then esterifies these acyl-CoAs into phosphatidylethanolamines (PEs). These PEs containing PUFAs are the direct substrates of lipid peroxidation (Zhang et al., 2022). All these findings suggest that Ponicidin-induced cell death was partly due to ferroptosis associated with mitochondrial membrane permeability.

To further investigate the mechanism underlying the beneficial effects of Ponicidin on Lenvatinib-resistant HCC cells, we used molecular docking, HuProt™ Human Proteome Microarray, and Co-IP to analyze the ferroptosis-related proteins that bind to Ponicidin. These analyses revealed that KEAP1 could bind to Ponicidin. KEAP1 acts as a negative regulator of NRF2. It binds to NRF2 through its Kelch domain, anchors NRF2 in the cytoplasm, and makes it in a state of being recognized and degraded by the proteasome, thus inhibiting the transcriptional activity of NRF2 (Suzuki et al., 2023). NRF2, the key anti-oxidative transcription

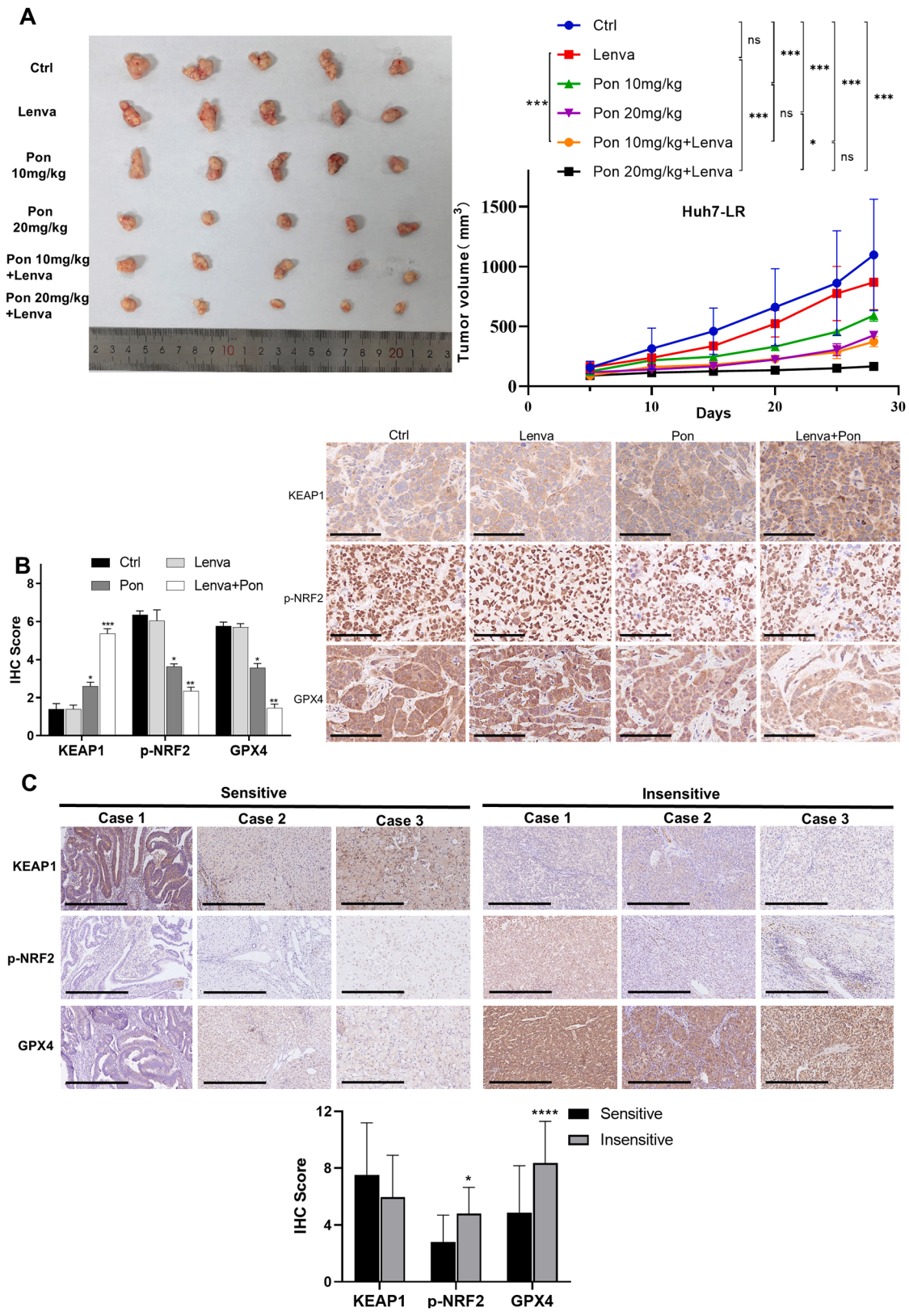

Fig. 6. Expression of KEAP1/NRF2/GPX4 in Lenvatinib-resistant mouse xenograft tumor models and patients. (A) The volumes of subcutaneous tumor tissues derived from mice in the control, 10 mg/kg Lenvatinib, 10 mg/kg Ponicidin, 20 mg/kg Ponicidin, and two combination groups ($n = 5$). (B) Tumors derived from the control, 10 mg/kg Lenvatinib, 20 mg/kg Ponicidin and the combination groups were immunostained for KEAP1, p-NRF2 and GPX4, Scale bar: 100 μm. (C) Immunohistochemical staining of liver cancer tissues from patients in the sensitive group ($n = 29$) and insensitive group ($n = 30$). Scale bar: 500 μm. All the results are shown as the mean ± SD. Two-way ANOVA was used to analyze the data; *$p < 0.05$, ** $p < 0.01$, *** $p < 0.001$, **** $p < 0.0001$.

Table 1
The associations of Lenvatinib sensitive or insensitive with clinicopathologic characteristics in 59 patients with HCC.

	Whole study(n = 59)		
	Lenvatinib sensitive (n = 29)	Lenvatinib insensitive (n = 30)	P
Sex			0.275
male	23	20	
Female	6	10	
Age(years)			0.003
<50	8	20	
≥50	21	10	
AFP (ng/ml)			0.005
≤400	7	18	
>400	22	12	
Tumor volume(cm^3)			0.145
<5	13	8	
≥5	16	22	
cirrhosis			0.497
no	18	16	
yes	11	14	
AJCC Stage			0.002
StageI-II	28	19	
Stage III-IV	1	11	
GPX4			0.000
low	10	0	
high	19	30	
KEAP1			0.959
low	4	4	
high	25	26	
p-NRF2			0.004
low	15	5	
high	14	25	

factor, plays a dominant role in defense machinery by reprogramming the iron, intermediate, GPX4-related network and the antioxidant system to attenuate ferroptosis (Jiang et al., 2024). Its downstream cytoprotective genes facilitate the maintenance of redox homeostasis (Kerins and Ooi, 2018). NRF2 activity is primarily regulated by KEAP1 and is essential for protecting cells from oxidative stress. Under normal conditions, NRF2 remains in the cytoplasm in an inactive complex with KEAP1. When cells are exposed to electrophiles or oxidative stress, electrophilic metabolites inhibit KEAP1 activity, causing NRF2 to dissociate from KEAP1 and translocate to the nucleus. In the nucleus, NRF2 forms a heterodimer with small MAF proteins and initiates antioxidant responses by activating downstream target genes (Srivastava et al., 2022). In this study, we confirmed that Ponicidin directly binded with KEAP1 and enhanced its protein stability, thereby inhibited NRF2 activation, similar to the effect of the NRF2 inhibitor ML385. These results suggest that Ponicidin's anti-tumor and drug-resistance reversal effects may be due to enhanced KEAP1-NRF2 binding, which prevents NRF2 from translocating to the nucleus and activating downstream responses (Fig. 7). This mechanistic insight represents a significant advance in ferroptosis regulation, as no previous studies have documented small-molecule natural products capable of counteracting therapeutic resistance through stabilization of the KEAP1-NRF2 interaction.

We also evaluated Ponicidin's anti-tumor efficacy *In vivo* using a Lenvatinib-resistant HCC cell-derived xenograft model. We observed that Ponicidin inhibited tumor growth, and tumor volume in the combination group was significantly reduced, indicating the synergistic effect of Lenvatinib and Ponicidin. Additionally, KEAP1 expression was upregulated, while NRF2 and GPX4 were downregulated by Ponicidin treatment in the Huh7-LR CDX model, indicating that the NRF2-GPX4 anti-ferroptosis pathway was inhibited and that this inhibition was reversed by Ponicidin. Clinically, we observed elevated p-NRF2 and GPX4 levels in Lenvatinib-insensitive HCC patients, directly linking ferroptosis suppression to therapeutic resistance in humans, a correlation previously unexplored. Importantly, the synergistic efficacy of Ponicidin and Lenvatinib *In vivo*, highlights its translational potential. However, clinical translation of Ponicidin requires careful consideration of its pharmacokinetic limitations and adverse effects. As a diterpenoid derived from Rabdosia rubescens, Ponicidin exhibits low solubility and poor oral bioavailability (absolute bioavailability 4.32–10.8 % in rats), severely restricting its clinical applicability (Xu et al., 2006). Furthermore, reported adverse reactions including gastrointestinal discomfort, hepatorenal toxicity, and cardiovascular abnormalities (Li et al., 2021) necessitate strategic optimization. Potential solutions to these limitations are emerging. One way is using AI-assisted drug design to make structural modification of Ponicidin to reduce its adverse reaction. Or

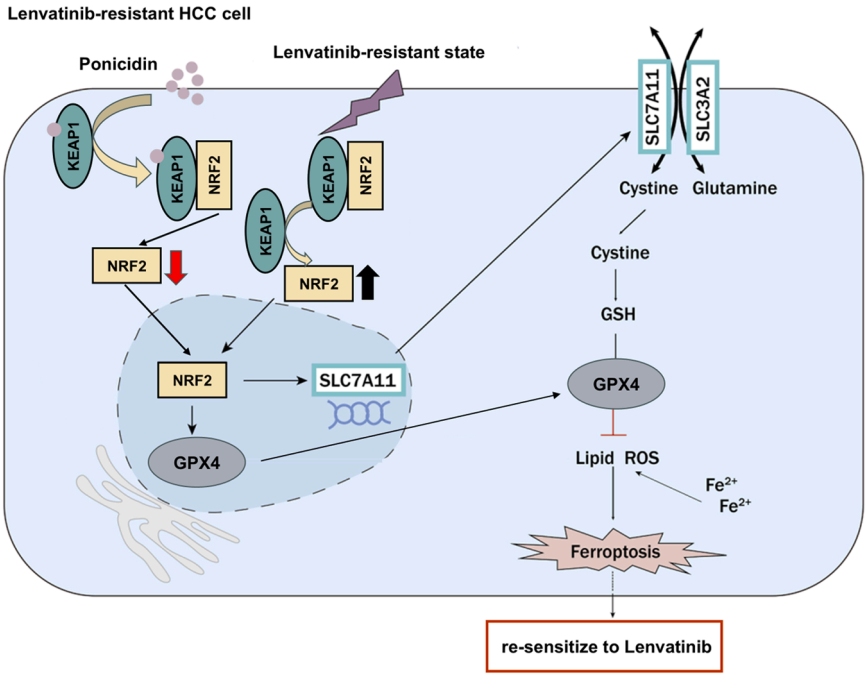

Fig. 7. A putative scheme illustrates the mechanism of ferroptosis induced by Ponicidin to enhance treatment sensitivity of Lenvatinib-resistant HCC cells.

preparing Ponicidin into liposomes and nanoparticles to change the distribution and metabolism in the body and thus reducing its side effects. Despite these challenges, our findings position Ponicidin as a uniquely promising candidate for drug resistant HCC management. Its multimodal effects, ferroptosis sensitization via KEAP1/NRF2 axis modulation, apoptosis induction, and synergy with TKIs, - address critical gaps in current HCC therapeutics. Collectively, our findings in conjunction with recent reports (Deng et al., 2024) represent a substantial breakthrough in ferroptosis regulation through stabilization of the KEAP1-NRF2 interaction, thereby establishing a novel framework for therapeutic intervention in liver diseases.

Conclusions

In conclusion, our studies identified a novel role for ferroptosis inhibition in the development of resistance to Lenvatinib therapy in HCC, potentially extending to patients. This work raises the possibility and provides the first proof of concept in mouse models, that targeting ferroptosis may be an effective strategy to overcome Lenvatinib therapy resistance. In fact, small-molecule drugs like Ponicidin are currently being explored as anti-cancer agents in preclinical stages. Our findings demonstrate that the direct binding of Ponicidin to KEAP1 reversed Lenvatinib resistance in Lenvatinib-resistant HCC. In summary, with Lenvatinib resistance representing a significant clinical challenge in HCC therapy, we provide the first preclinical evidence that Ponicidin could offer a promising approach to overcoming Lenvatinib resistance by inducing ferroptosis.

Ethics approval

All human samples were collected under an approved protocol by the Second Military Medical University Review Board (No. 82,322,055), and written informed consent was obtained from each donor. Animal welfare and experimental procedures were performed strictly in accordance with high standards for animal welfare and other related ethical regulations approved by the Shanghai University of Medicine and Health Sciences. Ethics approval for animal work (approval no 2022-SZR-18-450103198005091O4X) was provided by Animal Ethics Committee of Shanghai University of Medicine and Health Sciences at 10th Feb 2022.

CRediT authorship contribution statement

Lisha Zhang: Writing – original draft, Data curation, Conceptualization. **Hao Wang:** Writing – original draft, Formal analysis, Data curation. **Beibei Liang:** Methodology, Investigation, Formal analysis, Data curation. **Lijuan Qin:** Formal analysis, Data curation. **Mingzhu Zhang:** Methodology. **Xingxian Lv:** Methodology. **Shi Hu:** Software. **Xiaoyu Fan:** Data curation. **Wei Xie:** Resources. **Hao Yang:** Resources, Methodology. **Gang Huang:** Supervision, Funding acquisition. **Wei Jing:** Writing – review & editing, Methodology. **Jian Zhao:** Writing – review & editing, Funding acquisition, Conceptualization.

Declaration of competing interest

The authors declare that they have no known competing financial interests or personal relationships that could have appeared to influence the work reported in this paper.

Acknowledgement

The present study was supported by the National Natural Science Foundation of China (grant nos. 81972252, 81670573, 81830052, 82127807 and 82322055), the Shanghai Nature Science Foundation (grant no 21ZR1455900 and 22ZR1428000), the National Key Research and Development Program of China (grant no 2020YFA0909000) and the Construction Project of Shanghai Key Laboratory of Molecular Imaging (grant no 18DZ2260400).

Supplementary materials

Supplementary material associated with this article can be found, in the online version, at doi:10.1016/j.phymed.2025.156824.

References

Abdullah, N.A., Md Hashim, N.F., Ammar, A., Muhamad Zakuan, N., 2021. An insight into the anti-angiogenic and anti-metastatic effects of Oridonin: current knowledge and future potential. Molecules. 26.

Basit, F., van Oppen, L.M., Schockel, L., Bossenbroek, H.M., van Emst-de Vries, S.E., Hermeling, J.C., Grefte, S., Kopitz, C., Heroult, M., Hgm Willems, P., Koopman, W.J., 2017. Mitochondrial complex I inhibition triggers a mitophagy-dependent ROS increase leading to necroptosis and ferroptosis in melanoma cells. Cell Death. Dis. 8, e2716.

Bo, W., Chen, Y., 2023. Lenvatinib resistance mechanism and potential ways to conquer. Front. Pharmacol. 14, 1153991.

Cui, W., Zhang, J., Wu, D., Zhang, J., Zhou, H., Rong, Y., Liu, F., Wei, B., Xu, X., 2022. Ponicidin suppresses pancreatic cancer growth by inducing ferroptosis: insight gained by mass spectrometry-based metabolomics. Phytomedicine 98, 153943.

Deng, Y., Chu, X., Li, Q., Zhu, G., Hu, J., Sun, J., Zeng, H., Huang, J., Ge, G., 2024. Xanthohumol ameliorates drug-induced hepatic ferroptosis via activating Nrf2/xCT/GPX4 signaling pathway. Phytomedicine 126, 155458.

Dixon, S.J., Olzmann, J.A., 2024. The cell biology of ferroptosis. Nat. Rev. Mol. Cell Biol. 25, 424–442.

Du, J., Chen, C., Sun, Y., Zheng, L., Wang, W., 2015. Ponicidin suppresses HT29 cell growth via the induction of G1 cell cycle arrest and apoptosis. Mol. Med. Rep. 12, 5816–5820.

Friedmann Angeli, J.P., Schneider, M., Proneth, B., Tyurina, Y.Y., Tyurin, V.A., Hammond, V.J., Herbach, N., Aichler, M., Walch, A., Eggenhofer, E., Basavarajappa, D., Radmark, O., Kobayashi, S., Seibt, T., Beck, H., Neff, F., Esposito, I., Wanke, R., Forster, H., Yefremova, O., Heinrichmeyer, M., Bornkamm, G.W., Geissler, E.K., Thomas, S.B., Stockwell, B.R., O'Donnell, V.B., Kagan, V.E., Schick, J.A., Conrad, M., 2014. Inactivation of the ferroptosis regulator Gpx4 triggers acute renal failure in mice. Nat. Cell Biol. 16, 1180–1191.

Hassannia, B., Vandenabeele, P., Vanden Berghe, T., 2019. Targeting ferroptosis to iron out cancer. Cancer Cell 35, 830–849.

Hirose, W., Oshikiri, H., Taguchi, K., Yamamoto, M., 2022. The KEAP1-NRF2 system and esophageal cancer. Cancers. (Basel) 14.

Huang, Z., Xia, H., Cui, Y., Yam, J.W.P., Xu, Y., 2023. Ferroptosis: from basic research to clinical therapeutics in hepatocellular carcinoma. J. Clin. Transl. Hepatol. 11, 207–218.

Iseda, N., Itoh, S., Toshida, K., Tomiyama, T., Morinaga, A., Shimokawa, M., Shimagaki, T., Wang, H., Kurihara, T., Toshima, T., Nagao, Y., Harada, N., Yoshizumi, T., Mori, M., 2022. Ferroptosis is induced by lenvatinib through fibroblast growth factor receptor-4 inhibition in hepatocellular carcinoma. Cancer Sci. 113, 2272–2287.

Islam, M.T., Biswas, S., Bagchi, R., Khan, M.R., Khalipha, A.B.R., Rouf, R., Uddin, S.J., Shilpi, J.A., Bardaweel, S.K., Sabbah, D.A., Mubarak, M.S., 2019. Ponicidin as a promising anticancer agent: its biological and biopharmaceutical profile along with a molecular docking study. Biotechnol. Appl. Biochem. 66, 434–444.

Jang, S., Chapa-Dubocq, X.R., Tyurina, Y.Y., St Croix, C.M., Kapralov, A.A., Tyurin, V.A., Bayir, H., Kagan, V.E., Javadov, S., 2021. Elucidating the contribution of mitochondrial glutathione to ferroptosis in cardiomyocytes. Redox. Biol. 45, 102021.

Javadov, S., 2022. Mitochondria and ferroptosis. Curr. Opin. Physiol. 25.

Jiang, X., Yu, M., Wang, W.K., Zhu, L.Y., Wang, X., Jin, H.C., Feng, L.F., 2024. The regulation and function of Nrf2 signaling in ferroptosis-activated cancer therapy. Acta Pharmacol. Sin. 45, 2229–2240.

Jin, H., Shi, Y., Lv, Y., Yuan, S., Ramirez, C.F.A., Lieftink, C., Wang, L., Wang, S., Wang, C., Dias, M.H., Jochems, F., Yang, Y., Bosma, A., Hijmans, E.M., de Groot, M. H.P., Vegna, S., Cui, D., Zhou, Y., Ling, J., Wang, H., Guo, Y., Zheng, X., Isima, N., Wu, H., Sun, C., Beijersbergen, R.L., Akkari, L., Zhou, W., Zhai, B., Qin, W., Bernards, R., 2021. EGFR activation limits the response of liver cancer to lenvatinib. Nature 595, 730–734.

Kerins, M.J., Ooi, A., 2018. The roles of NRF2 in modulating cellular iron homeostasis. Antioxid. Redox. Signal. 29, 1756–1773.

Kudo, M., Finn, R.S., Qin, S., Han, K.H., Ikeda, K., Piscaglia, F., Baron, A., Park, J.W., Han, G., Jassem, J., Blanc, J.F., Vogel, A., Komov, D., Evans, T.R.J., Lopez, C., Dutcus, C., Guo, M., Saito, K., Kraljevic, S., Tamai, T., Ren, M., Cheng, A.L., 2018. Lenvatinib versus sorafenib in first-line treatment of patients with unresectable hepatocellular carcinoma: a randomised phase 3 non-inferiority trial. Lancet 391, 1163–1173.

Ladd, A.D., Duarte, S., Sahin, I., Zarrinpar, A., 2024. Mechanisms of drug resistance in HCC. Hepatology 79, 926–940.

Lei, G., Zhuang, L., Gan, B., 2022. Targeting ferroptosis as a vulnerability in cancer. Nat. Rev. Cancer 22, 381–396.

Li, X., Zhang, C.T., Ma, W., Xie, X., Huang, Q., 2021. Oridonin: a review of its pharmacology, pharmacokinetics and toxicity. Front. Pharmacol. 12, 645824.

Li, Z., Hu, Y., Zheng, H., Li, M., Liu, Y., Feng, R., Li, X., Zhang, S., Tang, M., Yang, M., Yu, R., Xu, Y., Liao, X., Chen, S., Qian, W., Zhang, Q., Tang, D., Li, B., Song, L., Li, J.,

2024. LPCAT1-mediated membrane phospholipid remodelling promotes ferroptosis evasion and tumour growth. Nat. Cell Biol. 26, 811–824.
Liu, J.J., Huang, R.W., Lin, D.J., Peng, J., Zhang, M., Pan, X., Hou, M., Wu, X.Y., Lin, Q., Chen, F., 2006. Ponicidin, an ent-kaurane diterpenoid derived from a constituent of the herbal supplement PC-SPES, Rabdosia rubescens, induces apoptosis by activation of caspase-3 and mitochondrial events in lung cancer cells in vitro. Cancer Invest. 24, 136–148.
Llovet, J.M., Zucman-Rossi, J., Pikarsky, E., Sangro, B., Schwartz, M., Sherman, M., Gores, G., 2016. Hepatocellular carcinoma. Nat. Rev. Dis. Primers. 2, 16018.
Pei, J., Pan, X., Wei, G., Hua, Y., 2023. Research progress of glutathione peroxidase family (GPX) in redoxidation. Front. Pharmacol. 14, 1147414.
Perelman, A., Wachtel, C., Cohen, M., Haupt, S., Shapiro, H., Tzur, A., 2012. JC-1: alternative excitation wavelengths facilitate mitochondrial membrane potential cytometry. Cell Death. Dis. 3, e430.
Qin, Y., Han, S., Yu, Y., Qi, D., Ran, M., Yang, M., Liu, Y., Li, Y., Lu, L., Liu, Y., Li, Y., 2024. Lenvatinib in hepatocellular carcinoma: resistance mechanisms and strategies for improved efficacy. Liver. Int. 44, 1808–1831.
Sanz, A.B., Sanchez-Nino, M.D., Ramos, A.M., Ortiz, A., 2023. Regulated cell death pathways in kidney disease. Nat. Rev. Nephrol. 19, 281–299.
Schlumberger, M., Tahara, M., Wirth, L.J., Robinson, B., Brose, M.S., Elisei, R., Habra, M. A., Newbold, K., Shah, M.H., Hoff, A.O., Gianoukakis, A.G., Kiyota, N., Taylor, M.H., Kim, S.B., Krzyzanowska, M.K., Dutcus, C.E., de las Heras, B., Zhu, J., Sherman, S.I., 2015. Lenvatinib versus placebo in radioiodine-refractory thyroid cancer. N. Engl. J. Med. 372, 621–630.
Song, X., Liu, J., Kuang, F., Chen, X., Zeh 3rd, H.J., Kang, R., Kroemer, G., Xie, Y., Tang, D., 2021. PDK4 dictates metabolic resistance to ferroptosis by suppressing pyruvate oxidation and fatty acid synthesis. Cell Rep. 34, 108767.
Srivastava, R., Fernandez-Gines, R., Encinar, J.A., Cuadrado, A., Wells, G., 2022. The current status and future prospects for therapeutic targeting of KEAP1-NRF2 and beta-TrCP-NRF2 interactions in cancer chemoresistance. Free Radic. Biol. Med. 192, 246–260.
Suzuki, T., Takahashi, J., Yamamoto, M., 2023. Molecular basis of the KEAP1-NRF2 signaling pathway. Mol. Cells 46, 133–141.
Xie, Y., Hou, W., Song, X., Yu, Y., Huang, J., Sun, X., Kang, R., Tang, D., 2016. Ferroptosis: process and function. Cell Death. Differ. 23, 369–379.
Xu, W., Sun, J., Zhang, T.T., Ma, B., Cui, S.M., Chen, D.W., He, Z.G., 2006. Pharmacokinetic behaviors and oral bioavailability of oridonin in rat plasma. Acta Pharmacol. Sin. 27, 1642–1646.
Yang, R., Gao, W., Wang, Z., Jian, H., Peng, L., Yu, X., Xue, P., Peng, W., Li, K., Zeng, P., 2024. Polyphyllin I induced ferroptosis to suppress the progression of hepatocellular carcinoma through activation of the mitochondrial dysfunction via Nrf2/HO-1/GPX4 axis. Phytomedicine 122, 155135.
Zhang, C., Liu, X., Jin, S., Chen, Y., Guo, R., 2022. Ferroptosis in cancer therapy: a novel approach to reversing drug resistance. Mol. Cancer 21, 47.
Zhang, Z., Xu, J., Liu, B., Chen, F., Li, J., Liu, Y., Zhu, J., Shen, C., 2019. Ponicidin inhibits pro-inflammatory cytokine TNF-alpha-induced epithelial-mesenchymal transition and metastasis of colorectal cancer cells via suppressing the AKT/GSK-3beta/snail pathway. Inflammopharmacology. 27, 627–638.